

GWT1 Gene Is Required for Inositol Acylation of Glycosylphosphatidylinositol Anchors in Yeast*

Received for publication, January 30, 2003, and in revised form, April 15, 2003
Published, JBC Papers in Press, April 24, 2003, DOI 10.1074/jbc.M301044200

Mariko Umemura‡, Michiyo Okamoto‡, Ken-ichi Nakayama‡, Koji Sagane§, Kappei Tsukahara§,
Katsura Hata§, and Yoshifumi Jigami‡†

From the ‡Research Center for Glycoscience, National Institute of Advanced Industrial Science and Technology,
Tsukuba Central 6, Higashi 1-1-1, Tsukuba, Ibaraki 305-8566 and §Tsukuba Research Laboratories, Eisai Co., Ltd.,
Tokodai 5-1-3, Tsukuba, Ibaraki 300-2635, Japan

Glycosylphosphatidylinositol (GPI) is a conserved post-translational modification to anchor cell surface proteins to plasma membrane in all eukaryotes. In yeast, GPI mediates cross-linking of cell wall mannoproteins to β 1,6-glucan. We reported previously that the GWT1 gene product is a target of the novel anti-fungal compound, 1-[4-butylbenzyl]isoquinoline, that inhibits cell wall localization of GPI-anchored mannoproteins in *Saccharomyces cerevisiae* (Tsukahara, K., Hata, K., Sagane, K., Watanabe, N., Kuromitsu, J., Kai, J., Tsuchiya, M., Ohba, F., Jigami, Y., Yoshimatsu, K., and Nagasu, T. (2003) *Mol. Microbiol.* 48, 1029–1042). In the present study, to analyze the function of the Gwt1 protein, we isolated temperature-sensitive *gwt1* mutants. The *gwt1* cells were normal in transport of invertase and carboxypeptidase Y but were delayed in transport of GPI-anchored protein, Gas1p, and were defective in its maturation from the endoplasmic reticulum to the Golgi. The incorporation of inositol into GPI-anchored proteins was reduced in *gwt1* mutant, indicating involvement of GWT1 in GPI biosynthesis. We analyzed the early steps of GPI biosynthesis *in vitro* by using membranes prepared from *gwt1* and $\Delta gwt1$ cells. The synthetic activity of GlcN-(acyl)PI from GlcN-PI was defective in these cells, whereas $\Delta gwt1$ cells harboring GWT1 gene restored the activity, indicating that GWT1 is required for acylation of inositol during the GPI synthetic pathway. We further cloned GWT1 homologues in other yeasts, *Cryptococcus neoformans* and *Schizosaccharomyces pombe*, and confirmed that the specificity of acyl-CoA in inositol acylation, as reported in studies of endogenous membranes (Franzot, S. P., and Doering, T. L. (1999) *Biochem. J.* 340, 25–32), is due to the properties of Gwt1p itself and not to other membrane components.

Many cell surface proteins are anchored in the lipid bilayer through glycosylphosphatidylinositol (GPI)¹ in mammalian

* The costs of publication of this article were defrayed in part by the payment of page charges. This article must therefore be hereby marked "advertisement" in accordance with 18 U.S.C. Section 1734 solely to indicate this fact.

The nucleotide sequence(s) reported in this paper has been submitted to the DDBJ/GenBank™/EBI Data Bank with accession number(s) AB092505.

† To whom correspondence should be addressed: Research Center for Glycoscience, National Institute of Advanced Industrial Science and Technology, Tsukuba Central 6, Higashi 1-1-1, Tsukuba, Ibaraki 305-8566, Japan. Tel.: 81-29-861-6160; Fax: 81-29-861-6161; E-mail: jigami.yoshi@aist.go.jp.

¹ The abbreviations used are: GPI, glycosylphosphatidylinositol; Ts⁻, temperature-sensitive; PI-PLC, phosphatidylinositol-specific phospholipase C; CoA, coenzyme A; BIQ, 1-[4-butylbenzyl]isoquinoline; ORF, open reading frame; GAPDH, glyceraldehyde-3-phosphate dehydrogenase; GFP, green fluorescent protein; ER, endoplasmic reticulum; CPY, carboxypeptidase Y; ConA, concanavalin A.

cells, yeast, and protozoa. GPI biosynthesis is essential for embryogenesis in mice and for growth of yeast cells (1) but not for growth of individual cells in mammals (2, 3). In the genome of budding yeast, *Saccharomyces cerevisiae*, ~60 open reading frames (ORFs) are predicted to encode GPI-anchored proteins (4). Most of these proteins are covalently linked to β 1,6-glucan of the cell wall component through the GPI portion (5, 6). Some of them, including Gas1p, are anchored to the plasma membrane (7). GPI-anchored proteins contain a signal peptide for secretion at the N terminus and a hydrophobic GPI attachment signal sequence at the C terminus (8).

GPI has the conserved core structure NH₂—CH₂—CH₂—PO₄—6Man α 1,2-Man α 1,6-Man α 1,4-GlcN α 1,6Ins-PO₄—lipid (9, 10). It is modified by addition of acyl chain to the inositol portion, and by addition of phosphoethanolamine to the first and possibly second mannose (Man) portion (11–13). Yeast and parasite, *Plasmodium falciparum*, have a modification in which α 1,2-linked Man is attached to the third Man of the above GPI core structure (14–16). After GPI maturation, which includes phosphoethanolamine attachment to the third and/or second Man, the modified GPI is transferred to the newly exposed C terminus of precursor proteins by transamidase. The resulting GPI-anchored proteins are efficiently packed into vesicles that are somewhat different from those containing other secretory proteins and that transported them to the Golgi (17–19). The lipid moiety is further remodeled to the ceramide, and the acyl chain of inositol is cleaved before lipid remodeling is completed (20, 21).

Inositol acylation has been reported mainly as palmitoylation at the 2-position of the inositol ring in yeast and mammalian cells (11, 22). This modification renders GPI precursors resistant to cleavage by phosphatidylinositol-specific phospholipase C (PI-PLC). Although inositol acylation occurs after mannosylation of GlcN-PI in the parasite *Trypanosoma brucei* (23, 24), it precedes mannosylation of GlcN-PI in yeast, mammalian cells, and *Plasmodium* (25, 26). These results were confirmed *in vivo* using mannose donor (dolichol-P-Man)-defective mutants that accumulate GlcN-(acyl)PI in yeast (27) and *in vitro* by a mannosylation/acylation assay with microsomal membranes using a synthetic substrate, dioctanoyl GlcN-PI in mammals (28). Yeast membranes utilize exogenous acyl-CoA as a donor in inositol acylation (29), whereas mouse cell membranes cannot utilize exogenous acyl-CoA as a donor, and acylation in mammalian cells requires GTP *in vitro* (30). *S. cerevisiae* membranes utilize acyl-CoA containing various lengths of fatty acid *in vitro* (22, 28), whereas *Cryptococcus neoformans* membranes have strict substrate specificity for acyl-CoA fatty acid length (28).

Most of the genes involved in GPI biosynthesis and GPI transfer to precursor proteins have been cloned and characterized (31–41), and show an amino acid sequence similarity

Inositol Acylation of Glycosylphosphatidylinositol in Yeast

between yeast and mammals. However, in the GPI biosynthetic pathway, the gene responsible for inositol acylation of GlcN-PI has not yet been identified, and it is unclear whether acylation precedes the "flip-flop" involving GPI translocation from the cytoplasmic side to luminal side of ER membranes (26). It is reported that de-acetylation, which precedes acylation, occurs on the cytoplasmic side, whereas the first mannosylation, which follows acylation, occurs on the luminal side of ER membranes (31, 33, 42). This raises the question whether inositol acylation occurs on the cytoplasmic or luminal side.

We recently reported (43) a novel compound, 1-[4-butylbenzyl]isoquinoline (BIQ), that inhibits cell wall localization of GPI-anchored mannosproteins in *S. cerevisiae*, and we identified a novel uncharacterized gene, *GWT1*, as a target of this compound. *GWT1* gene-deleted ($\Delta gwt1$) cells showed a defect in cell wall assembly and extremely slow growth. In the present study, we isolated temperature-sensitive mutants of *GWT1* (*gwt1*) to investigate the function of Gwt1p. Maturation and/or transport of the GPI-anchored protein, Gas1p, judged by the extent of glycosylation from the ER to Golgi, is impaired in the *gwt1* mutant. These findings suggest that *GWT1* may be involved in GPI biosynthesis, in GPI transfer to proteins, or in GPI-anchored protein transport from ER to Golgi. We also performed *in vitro* assay for the early steps of GPI biosynthesis by using membranes prepared from *gwt1* and $\Delta gwt1$ cells, and we confirmed that synthetic activity of GlcN-(acyl)PI from GlcN-PI during the GPI biosynthetic pathway is defective, *i.e.* *GWT1* is required for acylation of inositol in GPI biosynthesis.

EXPERIMENTAL PROCEDURES

Strains, Media, and Growth Conditions—Yeast strains used are listed in Table I. SD and YPD media were as described previously (44). Cells were grown in YPAD medium (1% yeast extract, 2% peptone, 2% glucose, 0.003% adenine) overnight at 24 °C as pre-culture. For invertase activity staining, cells were grown at 24 or 37 °C in YPA (1% yeast extract, 2% peptone, 0.003% adenine) containing 0.2% sucrose to induce invertase production. For pulse-chase experiments of Gas1p and CPY, cells were grown in SD medium with low SO₄²⁻ concentration (0.17% yeast nitrogen base without amino acid and ammonium sulfate, 5% glucose, nutrient supplements without cysteine and methionine, 0.5% casamino acid, 200 μM ammonium sulfate).

Low copy expression plasmid pRS315-GWT1 (pG), in which *S. cerevisiae* *GWT1* expressed under the native promoter, was constructed by using PCR to amplify a genomic DNA fragment containing *GWT1* and 1.4 kb immediately upstream of start codon and 1.2 kb immediately downstream of the *GWT1* coding region, and then cloning the fragment into low copy plasmid pRS315. Multicopy expression plasmid YEpl352-GWT1 (YG) was constructed by replacing the *GWT1* fragment of pRS315-GWT1 (pG) into the multicopy plasmid YEpl352. Constitutively high level expression plasmid pGAP-ScGWT1, in which expression of *GWT1* is under the control of GAPDH promoter, was made by using PCR to amplify the *GWT1* coding region, and cloning the fragment between GAPDH promoter and GAPDH terminator of the multicopy plasmid YEpl352GAPII, yielding pGAP-ScGWT1.

In Vitro Mutagenesis of GWT1 and Isolation of Temperature-sensitive *gwt1* Mutants—Temperature-sensitive (Ts⁻) alleles of *GWT1* were generated by PCR mutagenesis as described by Muhrlad *et al.* (45) and Maiti *et al.* (46). *GWT1* was amplified under mutagenic PCR conditions using forward primer (5'-TGTGCCTACAGAGCAGCCACTGCAAT-3') and reverse primer (5'-TCAACAACTAATGTACCTAGTAGGCAGGAG-3'). These PCRs contained the following components: 1× reaction buffer (Takara Shuzo); 50–100 ng of pRS315-GWT1 as template plasmid; 0.8 mM each primer; 2.5 mM MgCl₂; 0.5 mM each of dCTP, dGTP, and dTTP; 0.1 mM dATP; 5 units of LA Taq DNA polymerase (Takara Shuzo).

The mutagenized *GWT1* PCR product and a gapped plasmid were co-transformed into haploid strain ΔYG, which is a *gwt1* disrupted ($\Delta gwt1$) strain harboring YEpl352-GWT1 plasmid. The gapped plasmid was prepared by removing a 2012-bp *Sall-Bgl*III fragment of the *GWT1* gene in pRS315-GWT1 plasmid. Gap-repaired Leu⁺ transformants were transferred to medium containing 5-fluoroorotic acid to select YEpl352-GWT1 loss strains. Ura⁻ segregants were screened for temperature sensitivity at 37 °C into YPAD medium. The mutation points of

mutagenized *GWT1* plasmid on potential Ts⁻ mutants were determined by sequencing the coding region of *GWT1* gene.

Mutagenized *GWT1* was subcloned into an integration vector pRS304 or pRS306 and integrated into the *trp1* or *ura3* locus on the chromosome of WDG2, which is a *GWT1*/ $\Delta gwt1$ diploid strain (Table I). Trp⁺ or Ura⁺ transformants were selected, and His⁺, Trp⁺ or Ura⁺ and Ts⁻ segregants were identified after tetrad analysis.

Plasmid Construction of pGAP-GFP-ScGwt1-His—GFP-ScGwt1-His chimera cDNA was constructed by connecting each DNA fragment sequentially. The ORF of green fluorescent protein (GFP) in pEGFP-N2 (Clontech) was amplified by PCR with primers 5'-GGCGTCGAGACCAACCATGGTGAGCAAGGGCGAG-3' and 5'-GGTGAATTCTTGTACA-GCTCGTCCATGCCG-3'. *S. cerevisiae* *GWT1* ORF was amplified using the primers 5'-ACAGAATTCCACCATGTCGACTTTAAACAGAGAAAAGAGG-3' and 5'-TGTGGTACCTAGCTTAATGAATATTCTTTCTATCAA-3'. The His₆ epitope tag adaptor 5'-GGTACCGGAGGACATC-ATCATCATCATCATTAACGTACCCGGG-3' was added to the 3'-end of the GFP-ScGwt1 fusion construct. The resulting GFP-ScGwt1-His cassette was inserted into the low copy expression vector pRS314 or the multicopy expression vector YEpl352GAPII under the control of GAPDH promoter, yielding pRS314-GFP-ScGWT1 or pGAP-GFP-ScGWT1-His.

Fluorescence Microscopy—For imaging of GFP-ScGwt1-His fusion protein, cells grown to exponential phase were collected by centrifugation, fixed by 70% ethanol for 30 min, washed twice with distilled water, stained with 100 ng/ml 4',6-diamidino-2-phenylindole for 15 min, and visualized by fluorescence microscopy using an Olympus IX-70 fluorescence microscope system. Images were acquired by a digital charge-coupled device camera and processed by CoolSNAP software (Olympus).

Invertase Activity Staining—Cells were pre-cultured in 3 ml of YPAD medium at 24 or 37 °C and then transferred to YPA medium containing 0.2% sucrose to induce invertase expression. After 3 h of incubation at the indicated temperatures, the cells were collected, washed, and re-suspended in sample buffer (50 mM Tris-HCl, pH 6.8, 2% SDS, 6% 2-mercaptoethanol, 10% glycerol, bromophenol blue). Cells were broken by mixing with glass beads (425–600 μm, Sigma), and supernatants were recovered by centrifugation (13,000 × g). Then the samples were boiled and separated by SDS-PAGE. Mobility of invertase was detected by activity staining (47, 48).

Radiolabeling and Immunoprecipitation of Gas1p and CPY—Radiolabeling and immunoprecipitation were performed as described by Sutterlin *et al.* (17). Cells were grown to exponential phase in SD medium with low SO₄²⁻ concentration as described above, then collected by centrifugation, and replaced SD-SO₄²⁻ medium (0.17% yeast nitrogen base without amino acid and ammonium sulfate, 2% glucose and required nutrients without methionine and cysteine) by low sulfate medium. Samples were preincubated for 15 min at the indicated temperatures and then pulse-labeled with 3.7 MBq of Express ³⁵S-label (PerkinElmer Life Sciences) and chased. The chase was initiated by adding a 1/100 volume of chase liquid (0.3 M (NH₄)₂SO₄, 0.3% methionine, 0.3% cysteine). Samples were chased for various periods, and then Na₃N and NaF (10 mM final concentration) were added. Labeled cells were washed, resuspended in TEPI buffer (100 mM Tris-HCl, pH 7.5, 10 mM EDTA, proteinase inhibitors (Complete, Roche Applied Science)), and broken by mixing with glass beads (425–600 μm, Sigma) for 15 min at 4 °C. Cell lysates were solubilized by boiling with 1% SDS, combined with 1 ml of TNET buffer (100 mM Tris-HCl, pH 8, 100 mM NaCl, 5 mM EDTA, 1% Triton X-100), and centrifuged at 13,000 × g. Supernatants were incubated with anti-Gas1p (kindly provided by Dr. Howard Riezman) or anti-CPY (Molecular Probes) antibodies and protein G-agarose (Roche Applied Science) for 3 h. The beads were washed with TNET buffer and resuspended in SDS sample buffer. Immunoprecipitated samples were separated by SDS-PAGE and analyzed by Molecular Imager FX (Bio-Rad).

[³H]Inositol Labeling of Lipids and Proteins—Labeling of proteins and lipids with [³H]inositol was performed after cells were grown to exponential phase. Washed cells were resuspended in SD inositol-free medium containing 0.67% yeast nitrogen base without inositol and amino acid (Bio 101), 5% glucose, and nutrient supplements and then preincubated at the indicated temperature for 20 min. For labeling of lipids, myo-[2-³H]inositol (PerkinElmer Life Sciences) was added to the cell suspension and incubated for 1.5 h. Labeled lipids were extracted by shaking with glass beads (425–600 μm, Sigma) in CHCl₃/CH₃OH/water (10:10:3 v/v), and purified by n-butyl alcohol extraction. The lipids were analyzed by TLC with solvent system CHCl₃/CH₃OH/water (10:10:3 v/v). For labeling of proteins, myo-[1,2-³H]inositol (PerkinElmer Life Sciences) was added and incubated at the indicated temperature for 1.5 h, and the labeling reaction was stopped by adding Na₃N and NaF. Labeled proteins were extracted by shaking with glass

beads in TEPI buffer, and solubilized by boiling with 1% SDS. Samples were combined with ConA buffer containing 50 mM Tris-HCl, pH 7.5, 150 mM NaCl, 1 mM CaCl₂, 1 mM MnCl₂, and 1% Triton X-100 and centrifuged for 20 min at 4 °C at 13,000 × g. ConA-Sepharose (Amersham Bioscience) was added to the supernatants and incubated at 4 °C for 3 h. The Sepharose was washed with ConA buffer and then resuspended in SDS sample buffer. Samples were separated by SDS-PAGE and analyzed by Molecular Imager FX (Bio-Rad).

In Vitro Assay for the Early Steps of GPI Biosynthesis—To prepare ER-enriched membranes, cells were grown in YPAD medium at 24 °C overnight. The cell pellet was washed with TM buffer (50 mM Tris-HCl, pH 7.5, 2 mM MgCl₂). After centrifugation, the cells were homogenized by mixing with glass beads (425–600 µm, Sigma), and cell lysates were prepared by centrifugation at 1,000 × g to remove cell debris, nuclei, and intact cells. ER-enriched membrane fraction was prepared by centrifugation of cell lysates at 13,000 × g and used for the *in vitro* assay for GPI biosynthetic pathway, as described by Costello and Orlean (22). Mixed membranes were incubated in TM buffer containing 2 mM MnCl₂, 21 µg/ml tunicamycin, 10 µM nikkomycin, and 0.5 mM dithiothreitol, in the presence of 0.5–1 mM coenzyme A (CoA) and 1 mM ATP or 0.25 mM acyl-CoA. 4.44 kBq of UDP-[³C]GlcNAc (PerkinElmer Life Sciences) was added to start the reaction. After incubation for 1 h at 24 or 37 °C, the reaction was stopped by adding 1 ml of CHCl₃/CH₃OH (1:1 v/v), and the supernatant was separated and saved. The pellet was re-extracted by CHCl₃/CH₃OH/water (10:10:3 v/v). The lipid extracts were pooled, dried, and desalting by *n*-butyl alcohol extraction. Labeled lipid extracts were separated by TLC using Silica Gel 60 plate (Merck), with the solvent system CHCl₃/CH₃OH/1 M NH₄OH (10:10:3 v/v). Reaction products separated on TLC plates were detected by autoradiography and analyzed by Molecular Imager FX (Bio-Rad).

Enzyme Treatment of Radiolabeled Lipids—Radiolabeled lipids were treated with 0.5 units of PI-PLC prepared from *Bacillus thuringiensis* (ICN) in buffer containing 100 mM Tris-HCl, pH 7.5, and 0.2% Triton X-100. After incubation overnight at 37 °C, lipids were extracted with *n*-butyl alcohol and analyzed by TLC as described above.

Cloning of *C. neoformans* GWT1 Genes—Genome DNA and mRNA were purified from *C. neoformans* number 3 strain (49). In order to identify *C. neoformans* GWT1 gene (*CnGWT1*), we performed a sequence homology data base search by using highly conserved regions among the species as query. The search revealed that shotgun genome sequences (502042C05.x1) derived from “The *C. neoformans* Genome Sequencing Project” (<http://sequence-www.stanford.edu/group/C.neoformans/index.html>), and EST sequences (b6e06cn.f1) derived from “The *C. neoformans* cDNA Sequencing Project” (www.genome.ou.edu/cneo.html) were highly related to *S. cerevisiae* GWT1 (*ScGWT1*). Several primers were designed from the nucleotide information described above and were used to amplify *CnGWT1* by genomic PCRs. A combination of the primers GW61F (5'-GCCATAATAAGCTACCGAATTGCAATG-3') and GW52R (5'-CATTAACACCCATTGACAACCACG-3') amplified a single band of a 1.9-kb DNA fragment from *C. neoformans* genomic DNA. However, this fragment was partial and did not cover the C-terminal conserved sequences. To identify the downstream flanking sequences, we performed 3'-rapid amplification of cDNA ends using the 3'-rapid amplification of cDNA ends system (Invitrogen). 1.2 kb of cDNA fragment was amplified, using the gene-specific primer GW62F (5'-CATCTTGCGGTAGATTTGAAGTGTTC-3') and the Universal Amplification Primer included in the kit. Two additional primers, GW85F (5'-ATTGAAATTACCATGGGGATTACAAGT-CGGCCAAA-3') and GW87R (5'-CATGGTCGACACTTTAACATATCT-TGATCCTCC-3'), were designed to amplify the full-length *CnGWT1* gene. Approximately 2.0 kb of DNA fragment was obtained by PCR from genomic DNA, and 1.8 kb of *CnGWT1* cDNA was obtained by reverse transcriptase-PCR. Amplified *CnGWT1* cDNA was digested with EcoRI and SalI restriction enzymes and inserted into the yeast expression vector YEpl352GAPII for further analysis, yielding pGAP-CnGWT1.

Cloning of *Schizosaccharomyces pombe* GWT1 Gene—To clone the GWT1 homologue in *S. pombe* that was identified from the genome data base, YPD (Incyte Genomics, Inc.), genomic DNAs were purified from *S. pombe*. Several primers were designed from the nucleotide information described above. A combination of the primers, SpGWT1-F (5'-C-AATTGATGTACATAAAATTGGAAAAAGAAGCATTGTC-3') and SpGWT1-R (5'-GTCGACCTAAAGGCAAAACGAATTCCGT-3'), amplified a 1.38-kb DNA fragment from the *S. pombe* genomic DNA. This fragment is covered by the ORF of GWT1 homologue of *S. pombe* (*SpGWT1*). The amplified *SpGWT1* fragment was digested with *Mfe*I and *Sal*I restriction sites and inserted into the yeast expression vector YEpl352GAPII for further analysis, yielding pGAP-SpGWT1.

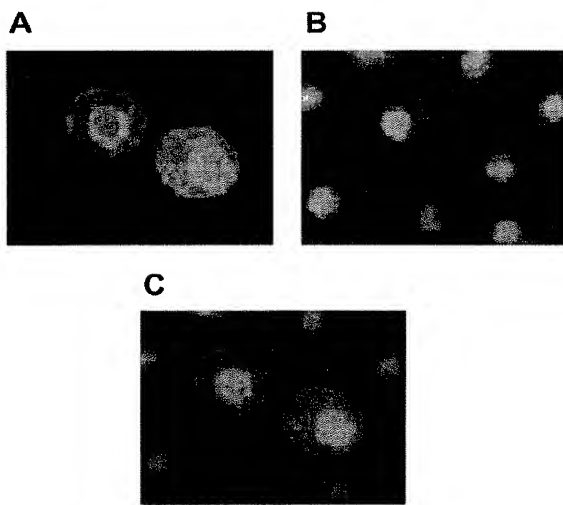


FIG. 1. Localization of GFP-Gwt1p. Wild type cells harboring the multicopy expression plasmid pGAP-GFP-ScGWT1-His (GFP-GWT1 strain, in Table I) were grown and visualized by fluorescence microscopy. *A*, localization of GFP-Gwt1p in ER. *B*, staining of DNA with 4',6-diamidino-2-phenylindole. *C*, merging of images in *A* and *B*.

RESULTS

GFP-Gwt1 Is Localized in the ER—We recently reported a novel anti-fungal compound, 1-[4-butylbenzyl]isoquinoline (BIQ), that blocks surface expression of GPI-anchored manno-proteins in *S. cerevisiae* (43) and identified the uncharacterized gene *GWT1* as a direct target of BIQ. To obtain information about Gwt1p function, we first tried using a low copy plasmid of the *GFP-ScGWT1* fusion gene to analyze its cellular localization, but this was unsuccessful because of the low expression level of the fusion gene. Instead, we used a multicopy plasmid of the *GFP-ScGWT1* fusion gene (pGAP-GFP-ScGWT1-His) to visualize Gwt1p by fluorescence microscopy. The expression plasmid was transformed into wild type cells, and transformed cells were grown to exponential phase.

As shown in Fig. 1, the GFP-ScGwt1-His fusion protein was detected at the peri-nuclear region characteristic of ER staining (50). We confirmed that the majority of the fusion protein (GFP-ScGwt1-His) was almost intact by immunoblot analysis using anti-GFP and anti-His antibodies (data not shown). Moreover, Gwt1 protein is a multiple transmembrane protein (43) and contains charged amino acid residues, such as aspartic acids, in its transmembrane regions, which is consistent with the prediction for ER retention or Golgi-ER retrieval of ER-localized membrane proteins (51). These results suggest that Gwt1p may be localized and may function in the ER.

Isolation of Temperature-sensitive *gwt1* Mutants—To address the function of Gwt1p, we attempted to isolate temperature-sensitive *gwt1* mutants from W303 background strain (Table I). We generated the mutant alleles by *in vitro* error-prone PCR of the *GWT1* fragment, followed by plasmid shuffling of generated *GWT1* gene, and we identified multiple missense mutations in each mutant allele. We determined which missense mutations caused the temperature-sensitive (Ts⁻) growth at 37 °C by replacing the fragment containing mutations with the corresponding fragment harboring wild type *GWT1* gene. Finally, we isolated three Ts⁻ mutant alleles (*gwt1-16*, *gwt1-20*, and *gwt1-28*), which contained only a few mutation points in the *GWT1* gene (Fig. 2*A*). Three amino acid substitutions (N330S, L362P, and V479A) and two amino acid substitutions (L209P and V259D) were identified as conferring Ts⁻ phenotype in *gwt1-16* and *gwt1-28*, respectively. The indi-

TABLE I
Yeast strains used in this study

Strain name	Plasmid	Genotype
G2-10		<i>MATa ura3-52 lys2-801 ade2-101 trp1-Δ1 his3-Δ200 leu2-Δ1 gwt1::his5⁺</i> G2-10
Δgwt1		<i>MATa ade2-1 his3-11 leu2-3,-112 trp1-1 ura3-1 can1-100</i>
W303-1A		<i>MATα ade2-1 his3-11 leu2-3,-112 trp1-1 ura3-1 can1-100</i>
W303-1B		<i>MATα/α ade2-1 ade2-1 his3-11 his3-11 leu2-3,-112 leu2-3,-112 trp1-1 trp1-1 ura3-1 ura3-1 can1-100 can1-100</i>
W303D		<i>GWT1/gwt1::his5⁺</i> W303D
WDG2		<i>W303-1A</i>
W303-v		<i>W303-1A</i>
GFP-GWT1	pRS315	<i>MATα gwt1::his5⁺ trp1::gwt1-16::TRP1</i> W303-1B
<i>gwt1-16</i>	pGAP-GFP-ScGWT1-His	<i>MATα gwt1::his5⁺ trp1::gwt1-20::TRP1</i> W303-1B
<i>gwt1-20</i>		<i>MATα gwt1::his5⁺ ura3::gwt1-28::URA3</i> W303-1B
<i>gwt1-28</i>		<i>gwt1-20</i>
<i>gwt1-v</i>		<i>gwt1-20</i>
<i>gwt1-pG</i>	pRS315	<i>MATα sec18-1 SUC2 mal gal2 CUP1</i>
HIMSF176	pRS315-GWT1 (pG)	<i>gwt1::his5⁺</i> W303-1A
Δ/YG	YEp352-GWT1 (YG)	<i>gwt1::his5⁺</i> W303-1A
Δ/pG	pRS315-GWT1 (pG)	<i>gwt1::his5⁺</i> W303-1A
YScGWT1	pGAP-ScGWT1	<i>gwt1::his5⁺</i> W303-1A
YCnGWT1	pGAP-CnGWT1	<i>gwt1::his5⁺</i> W303-1A
YSpGWT1	pGAP-SpGWT1	<i>gwt1::his5⁺</i> W303-1A

vidual single amino acid substitutions in the *gwt1-16* were not responsible for the Ts⁻ phenotype, suggesting the possibility that two or three independent amino acids may be responsible for the Ts⁻ phenotype. The revertant cells showing Ts⁺ phenotype appeared frequently at 37 °C in *gwt1-28*, probably due to a spontaneous mutation. These mutants were not suitable for further experiments. In *gwt1-20*, two amino acid substitutions (W63R and V64A) were responsible for Ts⁻ phenotype, whereas each single amino acid substitution did not show Ts⁻ phenotype (data not shown). Because the *gwt1-20* mutant contained only two vicinal amino acids substitutions, we used *gwt1-20* mutant for further analysis. The Ts⁻ phenotype of *gwt1-20* mutant was suppressed by the introduction of *GWT1* expression plasmid, pRS315-GWT1 (data not shown), indicating that the mutation of *gwt1-20* caused the *gwt1* loss of function.

To investigate the *gwt1-20* phenotype, we first checked the morphology of *gwt1-20* mutant at the non-permissive temperature (37 °C). Unlike wild type cells, *gwt1-20* mutants showed swelling and in some cases cell lysis (Fig. 2B). *gwt1-20* cells could not grow on YPD medium at 37 °C but did grow on YPD medium containing 1 M sorbitol, as osmotic stabilizer, at 37 °C. The growth defect of *gwt1-20* cells at 37 °C was also suppressed by the addition of 0.3 M KCl to the medium (data not shown). Because Δ*gwt1* cells showed a cell wall defect (43), we also further checked whether *gwt1-20* mutant cells were sensitive to SDS (52) or Calcofluor White (53), as another indication of cell wall defect. Fig. 2C shows that they were more sensitive to both compounds than were the wild type cells, indicating a cell wall defect.

There Are No General Defects in Secretory Pathway—Because the *gwt1-20* mutant showed a cell wall defect, it was most likely to show an alteration of protein secretion. To investigate whether protein secretion is altered in the *gwt1-20*, we analyzed invertase secretion, whose stage can be monitored based on molecular size due to the extent of glycosylation. ER-specific core-glycosylated invertase gives a small discrete band on SDS-PAGE. In Golgi, invertase is further glycosylated by outer chain mannosylation, giving a large diffuse band at a higher molecular weight on SDS-PAGE (48). Wild type, *gwt1-20*, and *sec18* mutant cells (Table I) were incubated at permissive (24 °C) or non-permissive (37 °C) temperatures, and invertase expression was induced. In *sec18* cells, core-glycosylated invertase was detected as a small discrete band at 37 °C due to the defect in protein transport from the ER to the

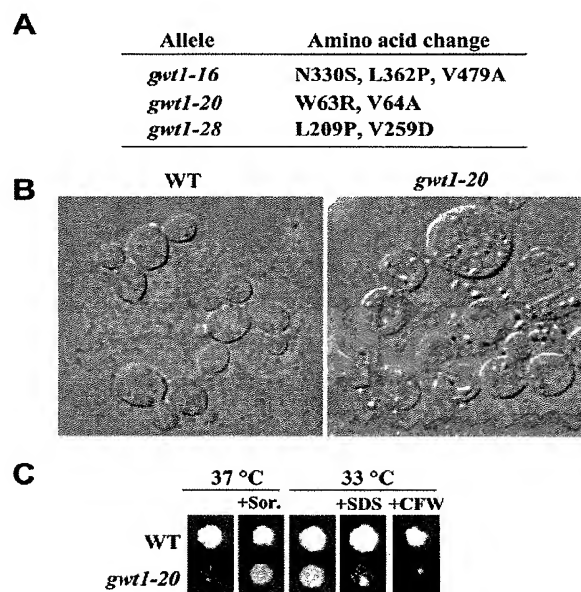


FIG. 2. Isolation and phenotype of *gwt1* mutants. A, mutational change in *gwt1* alleles. Details of isolation are described under "Experimental Procedures." B, morphology of *gwt1-20* mutant at 37 °C. Wild type (WT) and *gwt1-20* cells were grown to exponential phase at 25 °C in YPAD medium and then incubated at 37 °C for 8 h. Cell morphology was analyzed by microscopy. C, phenotype of *gwt1-20*. Wild type and *gwt1-20* cells were grown in YPAD medium. Diluted cells were spotted onto YPAD plate alone or with 1 M sorbitol (+Sor.), 0.005% SDS (+SDS), or 4 µg/ml Calcofluor White (+CFW). The plates were incubated for 2 days at the indicated temperatures.

Golgi. In contrast, invertase migrated at a higher molecular weight as diffuse in wild type and *gwt1-20* cells even at 37 °C (data not shown), indicating normal transport of invertase from ER to Golgi in these cells.

A soluble yeast vacuolar hydrolase, carboxypeptidase Y (CPY), is core-glycosylated in ER to generate the 67-kDa form (P1), and after transport to the Golgi, it is further glycosylated to generate the 69-kDa form (P2). Finally, after reaching the vacuole, CPY is processed to give a 61-kDa mature form (M) (54). Wild type and *gwt1-20* mutant cells were incubated at 24 or 37 °C, pulse-labeled with a mixture of [³⁵S]methionine and

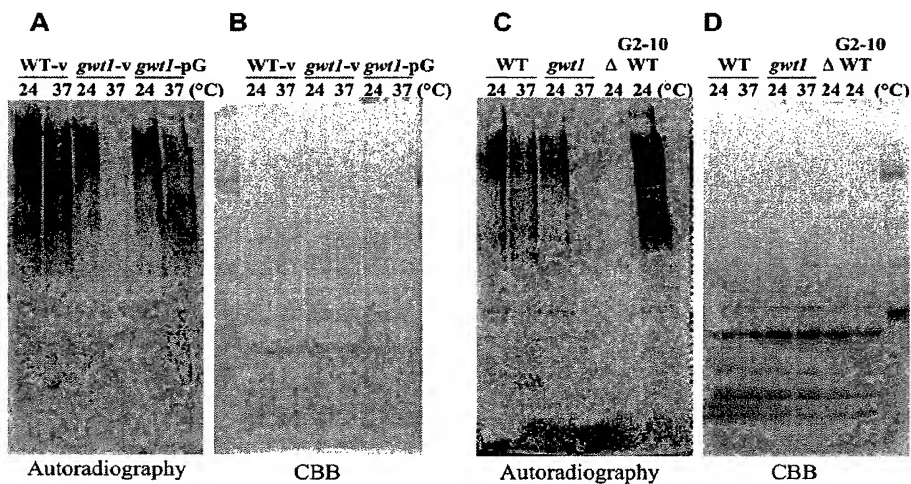


FIG. 3. Incorporation of radiolabeled inositol into proteins. Cells were preincubated in inositol-free medium at either 24 or 37 °C for 20 min and then labeled with myo-[1,2-³H]inositol for 60 min. The mannoprotein-enriched samples were purified by ConA-Sepharose from total lysates of labeled cells. Purified glycoprotein extracts were resolved by SDS-PAGE. Coomassie Brilliant Blue (CBB) staining confirmed the loaded amounts of proteins (B and D), and inositol incorporation was analyzed by autoradiography (A and C). A and B, wild type cells harboring the control vector (*WT-v*), *gwt1-20* mutant harboring the control vector (*gwt1-v*), and *gwt1-20* cells harboring the *GWT1* expression plasmid (*gwt1-pG*) in W303 strain background. C and D, wild type cells (WT) and *gwt1-20* cells (*gwt1*) in W303 strain background, Δ *gwt1* cells (Δ), and wild type cells (G2-10 WT) in G2-10 strain background.

[³⁵S]cysteine, and then chased for various periods, as described under “Experimental Procedures.” The cell lysates were subjected to immunoprecipitation with anti-CPY antibody and analyzed by SDS-PAGE. At both 24 and 37 °C, the extent of glycosylation and maturation of CPY was almost the same for *gwt1-20* cells as for wild type (data not shown), indicating that transport of CPY from ER to vacuole via Golgi was not altered in *gwt1-20* cells.

Gas1p is a hyperglycosylated GPI-anchored protein localized in the plasma membrane (7, 55) and has a core-glycosylated form of 105 kDa in the ER. After cleavage of the C-terminal peptide and subsequent attachment of GPI to the C-terminal processed polypeptide, GPI-anchored Gas1p is transported to Golgi, where Gas1p is converted to an extensively glycosylated 125-kDa mature form (56, 57). To investigate the transport of GPI-anchored proteins in the *gwt1-20* mutant, the cells were labeled with a mixture of [³⁵S]methionine and [³⁵S]cysteine and then chased, and the labeled cell lysates were immunoprecipitated with anti-Gas1p antibody. Gas1p remained mainly as the 105-kDa immature form at the non-permissive temperature (37 °C) in *gwt1-20* cells, unlike those in wild type cells (data not shown). These results suggest that the *gwt1-20* mutant may have a defect in Gas1p transport from ER to Golgi at the non-permissive temperature.

A previous study suggests that Gas1p maturation is affected by alteration in ceramide and subsequent sphingolipid synthesis (17, 58). To address the possibility that Gas1p maturation defect in *gwt1-20* at 37 °C results from alteration of ceramide, wild type and *gwt1-20* cells were labeled with myo-[2-³H]-inositol *in vivo*, and labeled lipid extracts were analyzed by TLC. There was no significant difference between *gwt1-20* versus wild type cells in sphingolipid levels (data not shown), indicating that there is some other reason for the Gas1p transport defect. These results indicate that *gwt1-20* cells have a defect in either GPI biosynthesis, GPI transfer to protein, or transport of GPI-anchored protein to the Golgi.

Incorporation of Radiolabeled Inositol to Proteins Is Defective in *gwt1-20* Mutant.—We investigated whether incorporation of radiolabeled inositol into proteins in *gwt1-20* mutant is blocked at 37 °C. All detectable protein-bound inositols are present as

the GPI-attached form in yeast (59). We labeled wild type, *gwt1-20*, and *sec18* cells with myo-[1,2-³H]inositol at 24 or 37 °C, and we prepared total cell lysates as described under “Experimental Procedures.” Radiolabeled glycoproteins were affinity-purified by ConA-Sepharose to enrich mannoproteins and separated by SDS-PAGE. The loaded amounts of total proteins were confirmed by Coomassie Brilliant Blue staining of the SDS-PAGE gel (Fig. 3, B and D). Labeled inositol was incorporated into proteins in *sec18* cells at the permissive temperature (24 °C), and the incorporation was not blocked at the non-permissive temperature (37 °C) despite the defect in protein transport from ER to Golgi, indicating that GPI transfer to proteins occurred normally in *sec18* even at 37 °C (data not shown). In contrast, in *gwt1-20* cells harboring a control vector pRS315 (*gwt1-v*), incorporation of labeled inositol into proteins was reduced slightly at 24 °C and was hardly detected at 37 °C (Fig. 3A). The *gwt1-20* cells harboring the *GWT1* expression plasmid (*gwt1-pG*) restored the incorporation signals into protein even at 37 °C (Fig. 3A), indicating that the defect is due to the loss of *gwt1* function. Moreover, the incorporation was reduced drastically in Δ *gwt1* (Δ), as compared with wild type (G2-10 WT) cells at 24 °C (Fig. 3C). These results indicate that the *gwt1-20* and Δ *gwt1* cells have a defect in either GPI biosynthesis or GPI anchor attachment to proteins.

In Vitro Assay of Early Steps in GPI Biosynthesis in *gwt1-20* Mutant.—To determine whether GPI biosynthesis is defective in *gwt1-20* cells, we checked enzyme activities of the early steps of the GPI biosynthetic pathway *in vitro*. Membrane fractions, prepared from wild type and *gwt1-20* cells grown to exponential phase, were incubated with UDP-[¹⁴C]GlcNAc at 24 °C, and lipid extracts containing the reaction products were separated by TLC. Membranes from wild type cells generated the three GPI intermediates, GlcNAc-PI, GlcN-PI, and GlcN-(acyl)PI, in the presence of CoA and ATP (Fig. 4A, lane 1). We treated the lipid extracts with PI-PLC at 37 °C overnight and confirmed that GlcN-(acyl)PI was resistant to the cleavage by PI-PLC, whereas the non-acylated intermediates, GlcNAc-PI and GlcN-PI, were not (Fig. 4A, lane 4). GlcN-(acyl)PI was not detected in the absence of CoA and ATP (Fig. 4A, lane 3), consistent with the previous finding that generation of acyl-CoA as a donor of

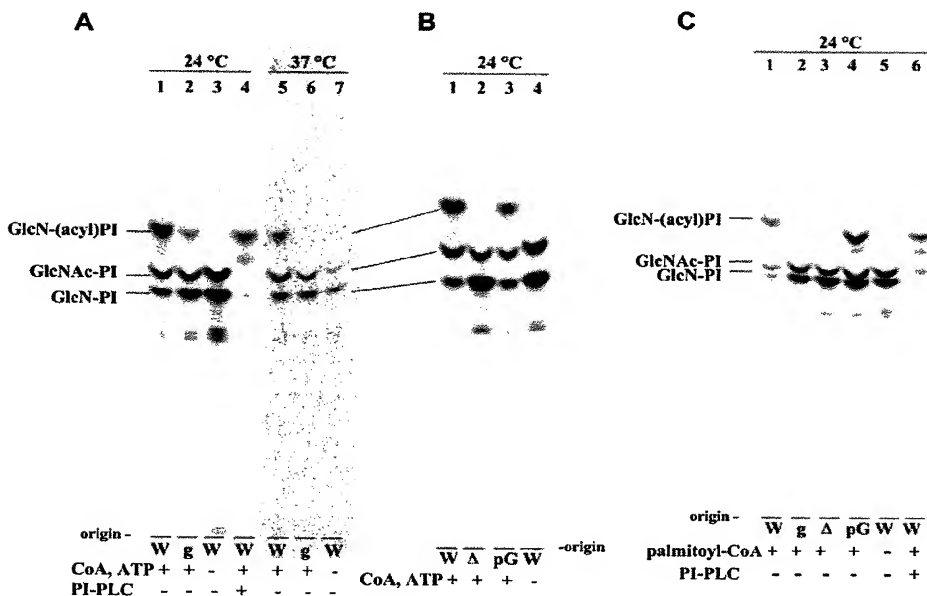


FIG. 4. *In vitro* assay of early steps in GPI biosynthesis. Membrane fractions were prepared by shaking the cells with glass beads and subjecting cells to centrifugation (see “Experimental Procedures”). Membranes were incubated for 1 h at the indicated temperature with UDP-[¹⁴C]GlcNAc in TM buffer containing the indicated acylation substrates, and labeled lipids were extracted and analyzed by TLC with solvent system CHCl₃/CH₃OH/1 M NH₄OH (10:10:3 v/v). *A*, assay of the membranes from wild type (*W*) and *gwt1-20* (*g*) cells grown at 24 °C. Samples were incubated in the presence of CoA and ATP at 24 or 37 °C. *B*, assay of membranes from wild type (*W*), *gwt1* disruptant (Δ), and *gwt1* disruptant cells harboring pRS315-GWT1 (*pG*) grown at 24 °C. *C*, assay of membranes from the same cells shown in *A* and *B* in the presence of 0.25 mM of palmitoyl-CoA.

inositol acylation from endogenous fatty acid requires CoA and ATP in *S. cerevisiae* (22). Interestingly, membranes prepared from *gwt1-20* cells generated much smaller amounts of GlcN-(acyl)PI than those from wild type cells, when measured at the permissive temperature (24 °C) (Fig. 4*A*, lane 2). In *gwt1-20* membranes measured at the non-permissive temperature (37 °C), GlcNAc-PI and GlcN-PI were detected, but the acylated product GlcN-(acyl)PI was not (Fig. 4*A*, lane 6). These results indicate that *gwt1-20* cells are defective in acylation of inositol during the GPI biosynthetic pathway. Moreover, we performed *in vitro* assay using membranes prepared from Δ *gwt1* cells. Although these membranes did not generate the acylated product GlcN-(acyl)PI (Fig. 4*B*, lane 2), such membranes prepared from Δ *gwt1* cells harboring the *GWT1* expression plasmid (Δ *pG*, as shown in Table I) showed normal inositol acyltransferase activity (Fig. 4*B*, lane 3). These results clearly indicate that *GWT1* is required for inositol acylation during GPI biosynthesis.

Palmitoyl-CoA is the major donor substrate for inositol acylation in GPI biosynthesis (11, 22). To address the possibility that the inositol acylation defect in *gwt1-20* cells may result from a defect in palmitoyl-CoA synthesis, we performed the above *in vitro* assay in the presence of palmitoyl-CoA as an exogenous substrate for acylation. Inositol acylation was still defective in membranes from *gwt1-20* cells, even when palmitoyl-CoA was added to the reaction mixture (Fig. 4*C*, lane 2). This finding indicates that *gwt1-20* mutation caused the defect in inositol acylation of GPI biosynthesis but not in acyl-CoA synthesis.

Cloning of *GWT1* Homologues from *S. pombe* and *C. neoformans*—The putative *GWT1* homologous genes of *S. pombe* and *C. neoformans* were identified in the respective genome project data bases. The *GWT1* homologue of *S. pombe* (*SpGWT1*) is termed *Spac144.10c*. This homologue consists of 459 amino acids and shows 35% homology with *GWT1* of *S. cerevisiae* (*ScGWT1*) (Fig. 6). The gene was obtained by PCR using

S. pombe genome as the template, and primers were designed from the genome (see “Experimental Procedures”). The PCR product of *GWT1* homologue was sequenced and confirmed to contain 1.38-kb ORF of *SpGWT1*.

Nucleotide sequences encoding the entire *C. neoformans* *Gwt1* protein were obtained by combination of genomic PCRs and reverse transcriptase-PCRs. Sequence analysis showed that the *C. neoformans* *GWT1* gene (*CnGWT1*) has three introns, and the deduced transcript encodes a protein with 598 amino acids. *C. neoformans* *Gwt1* protein has several additional regions ~30 amino acids in length, which are not observed in *S. cerevisiae* and *S. pombe* (Fig. 5). The nucleotide sequence data of *CnGWT1* reported in this paper were deposited in the DDBJ/EMBL/GenBank Data Libraries under the accession number AB092505.

These ORFs were cloned into YEpl352GAPII vector to construct expression plasmids, pGAP-*CnGWT1* and pGAP-*SpGWT1*, that were introduced into the Δ *gwt1* cells of *S. cerevisiae*. These genes suppressed the growth defect of Δ *gwt1* cells (data not shown). These cells also showed restoration of inositol acylation activity, which was defective in Δ *gwt1* cells of *S. cerevisiae* (Fig. 6, *B* and *C*), suggesting that they are the functional homologues of *ScGWT1*.

Substrate Specificity of Acyl-CoA in Inositol Acylation—Fatty acid from exogenous acyl-CoA can be directly transferred to inositol during *in vitro* inositol acylation of *S. cerevisiae* and *C. neoformans* using endogenous membranes (29). In contrast, it is considered that the transfer of fatty acid to inositol is not dependent on exogenous acyl-CoA in mammalian cells (30). Efficiency of inositol acylation differed for various fatty acids of acyl-CoA as the donor substrate between *S. cerevisiae* and *C. neoformans* (29), indicating that *C. neoformans* has stricter donor specificity than *S. cerevisiae*.

To investigate whether *GWT1* directly affects the above specificity, we performed *in vitro* inositol acylation assay in GPI biosynthesis and compared activities using membranes pre-

<i>S. cerevisiae</i>	WSTLWQKEDFVTGLNGGSITEINAVTSIAVITYISHNLK	41
<i>C. neoformans</i>	MGDYNSAKEENFVSDNPAGASINASINAVATYALMIAISPYIRHGLNNYLICVLPLL	60
<i>S. pombe</i>	MS-YKLEKAFAVSNTGSSSITCGLLIGIACNVLWNMT	40
<i>S. cerevisiae</i>	---	77
<i>C. neoformans</i>	---	120
<i>S. pombe</i>	---	74
<i>S. cerevisiae</i>	---	109
<i>C. neoformans</i>	AAGAAVSPVRLLPSCVAFASQSLSPDPTSMSPSSSSASGHEDPLCTMGVNRRRSIL	180
<i>S. pombe</i>	---	107
<i>S. cerevisiae</i>	---	141
<i>C. neoformans</i>	EGVSLDVPSHTDKVRISPVPYLRKKSRATKAQWVKENCRLPFLIVYRAHMMLTVICI	240
<i>S. pombe</i>	---	138
<i>S. cerevisiae</i>	LAVIDEPFPRNFAKVEIWGTSLMDLGVGFSFESNCIVSSRAT	188
<i>C. neoformans</i>	LAVIDEVPPWQCKCDEFGTSLMDLGVGFSFVFLGIVSRSKISPPPPPTPSSPAI	300
<i>S. pombe</i>	LAVIDEFLPFRYAKVEIWGTSLMDLGVGFSFESCTIVACKND	181
<i>S. cerevisiae</i>	IKSFKPSFLKNAFNALKSGCTLI	248
<i>C. neoformans</i>	FLGLLRLFPFVNLEYQEIVTEYGVHNFFITLSLPLV	360
<i>S. pombe</i>	IPLTPSPFTSLISRKSIPIITVLGFIRILMVGSIDPEHIVTEYGVHNFFITLAVPVLE	237
<i>S. cerevisiae</i>	LTFIDPVDTRAPRCSIAIFISCIYEWLLKKDRTLNLILADRNCFSANREGIFSFLGY	308
<i>C. neoformans</i>	AVGIRPLIQLRWSVLGVVIIHOLMITYLQSYFSGRSG	418
<i>S. pombe</i>	IFFLERRSLLKWSYFNLATEITLHHQCLVLTPL-FQKVALSPRTNLQAQREGIASLPGY	296
<i>S. cerevisiae</i>	CSIFLWQONTGYLIGNKPTINNYKPTSTDVAASKKSTWDYWTSTPI	368
<i>C. neoformans</i>	LSIEFLIGLSIQGDHVIR	473
<i>S. pombe</i>	-----I-SPPRERRVSETNEEHQSHPERKKLPLIMELCYSL	343
<i>S. cerevisiae</i>	TAIYFYGMYIISVWADR	423
<i>C. neoformans</i>	-----PLMYTRAESWKRFQRLLFPLICILIVLYLV	533
<i>S. pombe</i>	SNFLSVG	392
<i>S. cerevisiae</i>	FLVLSQLVFOYHPYSVSRRFANIPYTLIVLTYNLLFLTCYCLTDKIEGN	483
<i>C. neoformans</i>	GWALLGGWIWAGGEVSRRLANAPYVFWVVAAYNTFILLGIVLTHIPESPSTSQTSPSIL	593
<i>S. pombe</i>	VSRRSLVGVYVANVAFIIMFELTINILDAYLFP	452
<i>S. cerevisiae</i>	AECCLESINSNGIFLFTILANVSTGLVNMSWTDSSPLKSFVILAYCSF	490
<i>C. neoformans</i>	AVISVFLYR	598
<i>S. pombe</i>	VPPLIDAMNKGIAIFLAAANLITGLVNMSMKIYAPAWLISMGVUMLYLTLCSCVGWILKG	459
<i>S. cerevisiae</i>	VPKLLEDANNGLLVLFLIANVLTGVVNUISFDI	459
<i>C. neoformans</i>	LISSNARGLTMTMYLFICYMAHWLAQ	459
<i>S. pombe</i>	HQIRFRL	459

FIG. 5. Alignment of the putative amino acid sequence of Gwt1p from *S. cerevisiae*, *C. neoformans*, and *S. pombe*. Alignment of the Gwt1 proteins was generated using the ClustalW program (62). Black and gray boxes indicate identical and conserved amino acids, respectively. Underline indicates the additional sequences specific to *C. neoformans* Gwt1p.

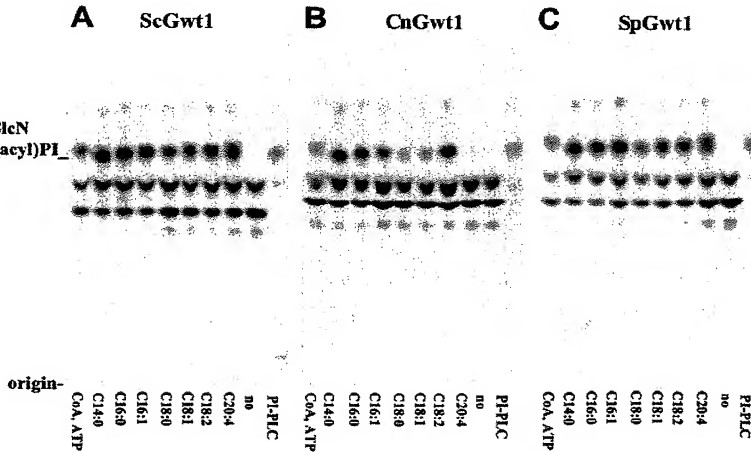


FIG. 6. Substrate specificity of acyl-CoA. Membranes prepared from *S. cerevisiae* *gwt1* disrupted cells harboring pGAP-ScGWT1 (A, YScGWT1), pGAP-CnGWT1 (B, YCnGWT1), and pGAP-SpGWT1 (C, YSpGWT1) plasmids were assayed for inositol acylation in the presence or absence of acyl-CoA or CoA and ATP as indicated (see "Experimental Procedures"). The *no lane* means no addition, and the *PI-PLC lane* means treatment by PI-PLC in the presence of CoA and ATP. Typical results from three independent experiments are shown.

pared from *S. cerevisiae* *Δgwt1* cells harboring pGAP-ScGWT1, pGAP-CnGWT1, and pGAP-SpGWT1 plasmids, respectively (YScGWT1, YCnGWT1, and YSpGWT1 strain, as shown in Table I). Addition of various acyl-CoAs stimulated the reaction and directly affected efficiency of GlcN-(acyl)PI formation in three yeast membranes (Fig. 6). Mobility of the acylation product GlcN-(acyl)PI on TLC differed slightly in response to polarity of the fatty acids, indicating that fatty acid of exogenous acyl-CoA was transferred directly to the inositol portion of GlcN-(acyl)PI.

To examine the substrate specificity of acyl-CoA, we compared the efficiency of inositol acylation by analyzing amounts

of acylated product GlcN-(acyl)PI on TLC (Fig. 6). Membranes of YScGWT1 or YSpGWT1 cells showed no significant difference in production of GlcN-(acyl)PI, regardless of which acyl-CoA was used as a donor (Fig. 6, A and C). In contrast, for the membrane of YCnGWT1 cells, myristoyl-CoA (C14:0) and linoleoyl-CoA (C18:2) were good substrates, whereas stearoyl-CoA (C18:0), oleoyl-CoA (C18:1), and arachidonoyl-CoA (C20:4) were poor substrates (Fig. 6B). These findings on acyl-CoA specificity were largely consistent with previous results on endogenous membranes (29) and indicate that the Gwt1 protein itself, not the other membrane components, determines acyl-CoA specificity in inositol acylation.

DISCUSSION

A novel uncharacterized gene, *GWT1*, was identified as a target of a novel compound that inhibits cell wall localization of GPI-anchored mannoproteins in *S. cerevisiae* (43). To address its function, we have analyzed a newly isolated *gwt1* Ts^- mutant that contains two vicinal amino acid substitutions (W63R and V64A) in Gwt1p. The cell wall defect was suggested by two observations, Calcofluor White sensitivity and suppression of Ts^- phenotype by the osmotic stabilizer (1 M sorbitol) (Fig. 2C), because these phenotypes were reported for many cells defective in various aspects of cell wall biosynthesis (48, 60). We showed here that the *gwt1* mutant was delayed in the ER-Golgi transport of the GPI-anchored protein, Gas1p, and drastically reduced the incorporation of radiolabeled inositol into proteins. Consequently, the observed delay of Gas1p transport in *gwt1* mutant may be due to the defects of GPI transfer to protein. Our results suggest that in the *gwt1* mutant, other GPI-anchored proteins, such as cell wall localized mannoproteins, may also show defects of GPI anchor attachment to proteins, impaired assembly to cell wall, and cause a cell wall defect.

The *gwt1* mutant is defective in inositol acylation in GPI biosynthesis, providing a possible explanation for a defect of GPI-anchored proteins in the *gwt1* mutant. Although incorporation of labeled inositol to protein was greatly reduced in *gwt1* mutant, the labeled signals were not completely diminished at 37 °C (Fig. 3), suggesting that GPI biosynthesis and GPI anchor attachment may not be blocked completely in the *gwt1*-20 mutant at the non-permissive temperature. Although inositol acylation products were not detected at 37 °C in the assay of early steps of GPI biosynthesis pathway (Fig. 4), the GPI biosynthesis may still function in *gwt1* living cells.

The *gwt1*-disrupted ($\Delta gwt1$) cells are viable in the G2-10 strain background, despite extremely slow growth. The $\Delta gwt1$ cells have defects in GPI transfer to proteins and GPI biosynthesis (Figs. 3 and 4B). We initially thought that blocking of inositol acylation might cause a total block of GPI biosynthesis and GPI anchor attachment to proteins. Recently, it was also reported that in the protozoan *P. falciparum*, GlcN inhibits inositol acylation of GPI, blocking GPI biosynthesis and cell growth (61). In contrast, because $\Delta gwt1$ cells are viable in the G2-10 strain background and lethal in the W303 strain background, we hypothesized that the GPI biosynthesis may still function without inositol acylation. It was reported that mannosylation of GPI core was not completely stopped in the absence of inositol acylation of GlcN-PI (28). Furthermore, the results that the acyl moiety on inositol ring is removed during the lipid remodeling (20, 21) suggest that *GWT1* may be different from other essential genes involved in GPI core structure synthesis in its function for cell viability. Further studies on the structural analysis of the accumulated GPI intermediates in *gwt1* mutant will provide the answer in the future.

No genes have been cloned and characterized so far for the unique step of inositol acylation during GPI biosynthesis in any eukaryotes from yeasts to mammals. We have shown here that *GWT1* is involved in this step, using *gwt1* mutant and $\Delta gwt1$ cells harboring *GWT1* expression plasmid (Fig. 4). The result on GFP-Gwt1 protein localization in the ER (Fig. 1), which is detectable only in the multicopy expression but not in the single copy expression due to the lack of sensitivity, supports the above conclusion, because the proteins involved in the synthesis of GPI core structure are known to reside in the ER (26). Our finding that addition of exogenous acyl-CoA did not suppress the defect of acylation activity in *gwt1* mutant (Fig. 4C) excludes the possibility that *GWT1* might encode acyl-CoA synthetase. We confirmed that *GWT1* itself determines the substrate specificity of inositol acylation of GPI, differences of

which were reported in *S. cerevisiae* and *C. neoformans* (29). The substrate specificity of inositol acylation examined by using the membranes prepared from *ScGWT1*- and *CnGWT1*-transformed cells (Fig. 6, A and B) was substantially the same as that reported previously (29) in studies of endogenous microsomal membranes prepared from various yeast species. We also tested substrate specificity of *SpGWT1* (Fig. 6C), which was mostly the same as that of *ScGWT1*. The differences in substrate specificity between *S. cerevisiae* and *C. neoformans* reflected the different properties of *GWT1* itself, because specificity was compared under the same cell background except for the origin of the *GWT1* gene. Interestingly, *C. neoformans* Gwt1p has several additional regions ~30 amino acids in length, in contrast to other Gwt1 proteins (Fig. 5). This insert may define the unique substrate specificity of inositol acylation in *C. neoformans*, which poorly utilizes stearoyl-CoA (C18:0), oleoyl-CoA (C18:1), and arachidonoyl-CoA (C20:4) (Fig. 6B). The substrate specificity of mammalian acylation enzyme is not reported, because it cannot utilize exogenous acyl-CoA as a donor (30). These differences in the inositol acylation of GPI in yeast may provide a good target for drugs directed against the pathogenic yeasts, such as *Candida albicans* and *C. neoformans*, that do not impair the inositol acylation in human. Because the Gwt1 protein (*i.e.* inositol acyltransferase) was a direct target for BIQ that was screened for anti-fungal compound, further study will be necessary to elucidate the molecular mechanism on the inhibition of inositol acylation by BIQ.

In conclusion, we have demonstrated that the *GWT1* gene is involved in inositol acylation of GPI biosynthesis, and Gwt1p is responsible for the substrate specificity of acylation. The function of inositol acylation in GPI biosynthetic pathway, especially in flip-flop of GPI and assembly of GPI-anchored proteins to plasma membrane and cell wall, is an important topic of future study. Because the acyl moiety on inositol is removed during the course of lipid remodeling (20, 21), it is also interesting to examine the role of inositol acylation in this process.

Acknowledgments—We are grateful to Dr. Howard Riezman (Biozentrum of the University of Basel) for providing anti-Gas1p antibody. We thank Drs. Sen-itiro Hakomori and Stephen Anderson (Pacific Northwest Research Institute) for critical reading of the manuscript and helpful discussions. We also thank Drs. Naoaki Watanabe and Yasutaka Takase (Eisai Co., Ltd.) for constructing the plasmids and PCR mutagenesis method, respectively. We are grateful to the *C. neoformans* cDNA Sequencing Project (Bruce A. Roe, Doris Kupfer, Heather Bell, Sun So, Yung Tang, Jennifer Lewis, Sola Yu, Kent Buchanan, Dave Dyer, and Juneann Murphy), supported by NIAID Grant AI147079 from the National Institutes of Health; the *C. neoformans* Genome Project at Stanford Genome Technology Center, supported by NIAID Grant U01 AI47087 from the National Institutes of Health; and the Institute for Genomic Research, supported by NIAID Grant U01 AI48594 from the National Institutes of Health.

REFERENCES

- Leidich, S. D., Drapp, D. A., and Orlean, P. (1994) *J. Biol. Chem.* **269**, 10193–10196
- Hyman, R. (1988) *Trends Genet.* **4**, 5–8
- Hirose, S., Mohney, R. P., Mutka, S. C., Ravi, L., Singleton, D. R., Perry, G., Tartakoff, A. M., and Medof, M. E. (1992) *J. Biol. Chem.* **267**, 5272–5278
- Caro, L. H., Tettelin, H., Vossen, J. H., Ram, A. F., van den Ende, H., and Klis, F. M. (1997) *Yeast* **13**, 1477–1489
- Smits, G. J., van den Ende, H., and Klis, F. M. (2001) *Microbiology* **147**, 781–794
- Shahinian, S., and Bussey, H. (2000) *Mol. Microbiol.* **35**, 477–489
- Nuoffer, C., Jeno, P., Conzelmann, A., and Riezman, H. (1991) *Mol. Cell. Biol.* **11**, 27–37
- Udenfriend, S., and Kodukula, K. (1995) *Annu. Rev. Biochem.* **64**, 563–591
- Puoti, A., and Conzelmann, A. (1992) *J. Biol. Chem.* **267**, 22673–22680
- McConville, M. J., and Ferguson, M. A. (1993) *Biochem. J.* **294**, 305–324
- Roberts, W. L., Myher, J. J., Kuksis, A., Low, M. G., and Rosenberry, T. L. (1988) *J. Biol. Chem.* **263**, 18766–18775
- Hirose, S., Prince, G. M., Sevlever, D., Ravi, L., Rosenberry, T. L., Ueda, E., and Medof, M. E. (1992) *J. Biol. Chem.* **267**, 16968–16974
- Kamitani, T., Menon, A. K., Hallaq, Y., Warren, C. D., and Yeh, E. T. (1992) *J. Biol. Chem.* **267**, 24611–24619
- Sipos, G., Puoti, A., and Conzelmann, A. (1994) *EMBO J.* **13**, 2789–2796

Inositol Acylation of Glycosylphosphatidylinositol in Yeast

23647

15. Grimme, S. J., Westfall, B. A., Wiedman, J. M., Taron, C. H., and Orlean, P. (2001) *J. Biol. Chem.* **276**, 27731–27739
16. Gerold, P., Dieckmann-Schuppert, A., and Schwarz, R. T. (1994) *J. Biol. Chem.* **269**, 2597–2606
17. Sutterlin, C., Doering, T. L., Schimmoller, F., Schroder, S., and Riezman, H. (1997) *J. Cell Sci.* **110**, 2703–2714
18. Muniz, M., Mor somme, P., and Riezman, H. (2001) *Cell* **104**, 313–320
19. Friedmann, E., Salzberg, Y., Weinberger, A., Shaltiel, S., and Gerst, J. E. (2002) *J. Biol. Chem.* **277**, 35274–35281
20. Reggiori, F., Canivenc-Gansel, E., and Conzelmann, A. (1997) *EMBO J.* **16**, 3506–3518
21. Chen, R., Walter, E. I., Parker, G., Lapurga, J. P., Millan, J. L., Ikehara, Y., Udenfriend, S., and Medof, M. E. (1998) *Proc. Natl. Acad. Sci. U. S. A.* **95**, 9512–9517
22. Costello, L. C., and Orlean, P. (1992) *J. Biol. Chem.* **267**, 8599–8603
23. Guther, M. L., and Ferguson, M. A. (1995) *EMBO J.* **14**, 3080–3093
24. Smith, T. K., Sharma, D. K., Crossman, A., Dix, A., Brimacombe, J. S., and Ferguson, M. A. (1997) *EMBO J.* **16**, 6667–6675
25. Gerold, P., Jung, N., Azzouz, N., Freilberg, N., Kobe, S., and Schwarz, R. T. (1999) *Biochem. J.* **344**, 731–738
26. Kinoshita, T., and Inoue, N. (2000) *Curr. Opin. Chem. Biol.* **4**, 632–638
27. Urakaze, M., Kamitani, T., DeGasperi, R., Sugiyama, E., Chang, H. M., Warren, C. D., and Yeh, E. T. (1992) *J. Biol. Chem.* **267**, 6459–6462
28. Doerler, W. T., Ye, J., Falck, J. R., and Lehrman, M. A. (1996) *J. Biol. Chem.* **271**, 27031–27038
29. Franzot, S. P., and Doering, T. L. (1999) *Biochem. J.* **340**, 25–32
30. Stevens, V. L., and Zhang, H. (1994) *J. Biol. Chem.* **269**, 31397–31403
31. Watanabe, R., Ohishi, K., Maeda, Y., Nakamura, N., and Kinoshita, T. (1999) *Biochem. J.* **339**, 185–192
32. Gaynor, E. C., Mondesert, G., Grimme, S. J., Reed, S. I., Orlean, P., and Emr, S. D. (1999) *Mol. Biol. Cell* **10**, 627–648
33. Maeda, Y., Watanabe, R., Harris, C. L., Hong, Y., Ohishi, K., Kinoshita, K., and Kinoshita, T. (2001) *EMBO J.* **20**, 250–261
34. Yan, B. C., Westfall, B. A., and Orlean, P. (2001) *Yeast* **18**, 1383–1389
35. Canivenc-Gansel, E., Imhof, I., Reggiori, F., Burda, P., Conzelmann, A., and Benachour, A. (1998) *Glycobiology* **8**, 761–770
36. Hamburger, D., Egerton, M., and Riezman, H. (1995) *J. Cell Biol.* **129**, 629–639
37. Benghezal, M., Benachour, A., Rusconi, S., Aebi, M., and Conzelmann, A. (1996) *EMBO J.* **15**, 6575–6583
38. Hiroi, Y., Komuro, I., Chen, R., Hosoda, T., Mizuno, T., Kudoh, S., Georgescu, S. P., Medof, M. E., and Yazaki, Y. (1998) *FEBS Lett.* **421**, 252–258
39. Ohishi, K., Inoue, N., Maeda, Y., Takeda, J., Riezman, H., and Kinoshita, T. (2000) *Mol. Biol. Cell* **11**, 1523–1533
40. Fraering, P., Imhof, I., Meyer, U., Strub, J. M., van Dorsselaer, A., Vionnet, C., and Conzelmann, A. (2001) *Mol. Biol. Cell* **12**, 3295–3306
41. Ohishi, K., Inoue, N., and Kinoshita, T. (2001) *EMBO J.* **20**, 4088–4098
42. Nakamura, N., Inoue, N., Watanabe, R., Takahashi, M., Takeda, J., Stevens, V. L., and Kinoshita, T. (1997) *J. Biol. Chem.* **272**, 15834–15840
43. Tsukahara, K., Hata, K., Sagane, K., Watanabe, N., Kuromitsu, J., Kai, J., Tsuchiya, M., Ohba, F., Jigami, Y., Yoshimatsu, K., and Nagasu, T. (2003) *Mol. Microbiol.* **48**, 1029–1042
44. Ausubel, F. M., Brent, R., Kingston, R. E., Moore, D. D., Seidman, J. G., Smith, J. A., and Struhl, K. (1999) *Short Protocols in Molecular Biology*, 4th Ed., 13–2–13–7, John Wiley & Sons, Inc., New York
45. Muhrad, D., Hunter, R., and Parker, R. (1992) *Yeast* **8**, 79–82
46. Maiti, T., Das, S., and Maitra, U. (2000) *Gene (Amst.)* **244**, 109–118
47. Gabriel, O., and Wang, S. F. (1969) *Anal. Biochem.* **27**, 545–554
48. Nagasu, T., Shimma, Y., Nakanishi, Y., Kuromitsu, J., Iwama, K., Nakayama, K., Suzuki, K., and Jigami, Y. (1992) *Yeast* **8**, 535–547
49. Hata, K., Kimura, J., Miki, H., Toyosawa, T., Nakamura, T., and Katsu, K. (1996) *Antimicrob. Agents Chemother.* **40**, 2237–2242
50. Sato, K., Sato, M., and Nakano, A. (2001) *J. Cell Biol.* **152**, 935–944
51. Delorenzi, M., Sexton, A., Shams-Eldin, H., Schwarz, R. T., Speed, T., and Schofield, L. (2002) *Infect. Immun.* **70**, 4510–4522
52. Shimizu, J., Yoda, K., and Yamasaki, M. (1994) *Mol. Gen. Genet.* **242**, 641–648
53. Lussier, M., White, A. M., Sheraton, J., di Paolo, T., Treadwell, J., Southard, S. B., Horenstein, C. I., Chen-Weiner, J., Ram, A. F., Kapteyn, J. C., Roemer, T. W., Vo, D. H., Bondoc, D. C., Hall, J., Zhong, W. W., Sdicu, A. M., Davies, J., Klis, F. M., Robbins, P. W., and Bussey, H. (1997) *Genetics* **147**, 435–450
54. Stevens, T., Esmon, B., and Schekman, R. (1982) *Cell* **30**, 439–448
55. Conzelmann, A., Riezman, H., Desponds, C., and Bron, C. (1988) *EMBO J.* **7**, 2233–2240
56. Fankhauser, C., and Conzelmann, A. (1991) *Eur. J. Biochem.* **195**, 439–448
57. Nuoffer, C., Horvath, A., and Riezman, H. (1993) *J. Biol. Chem.* **268**, 10558–10563
58. Horvath, A., Sutterlin, C., Manning-Krieg, U., Movva, N. R., and Riezman, H. (1994) *EMBO J.* **13**, 3687–3695
59. Conzelmann, A., Fankhauser, C., and Desponds, C. (1990) *EMBO J.* **9**, 653–661
60. Ram, A. F., Wolters, A., Ten Hoopen, R., and Klis, F. M. (1994) *Yeast* **10**, 1019–1030
61. Naik, R. S., Krishnegowda, G., and Gowda, C. D. (2002) *J. Biol. Chem.* **278**, 2036–2042
62. Thompson, J. D., Higgins, D. G., and Gibson, T. J. (1994) *Nucleic Acids Res.* **22**, 4673–4680